

Appendix: **Variation In Shape And Consistency Of Selection Between Populations Of The
New Zealand Hihi.**

Supplementary Information 1: Descriptions of the breeding dataset.

Note that the number of breeding attempts also correspond to the number of females reproducing each year as all clutches from a same female are considered as a combined annual breeding attempt (see main manuscript). A breeding attempt value of e.g., 15 therefore means that 15 females tried to reproduce at least once.

Table S.1. Breeding attempts recorded each year

Year	Tiritiri Mātangi		Kārori
	Number of breeding attempts	Number of breeding attempts	
1997	14		NA
1998	12		NA
1999	17		NA
2000	26		NA
2001	32		NA
2002	30		NA
2003	42		NA
2004	52		NA
2005	53		17
2006	64		15
2007	63		12
2008	70		18
2009	77		16
2010	94		18
2011	64		20
2012	75		13
2013	55		17
2014	53		27
2015	51		32
2016	62		25
2017	54		26
2018	67		19
2019	77		13

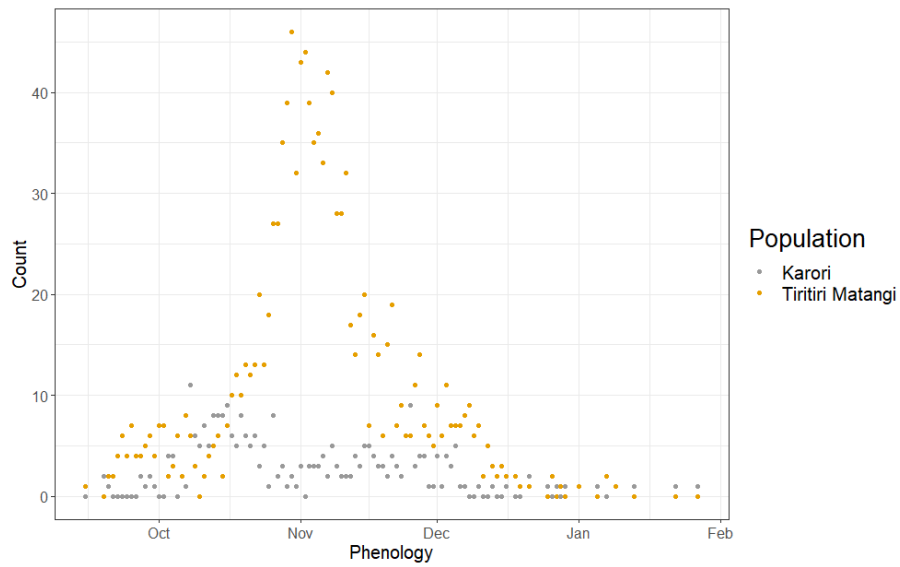


Fig.S.1.a. Number of laying events per date across the years in Tiritiri Mātangi and Kārori hihi populations.

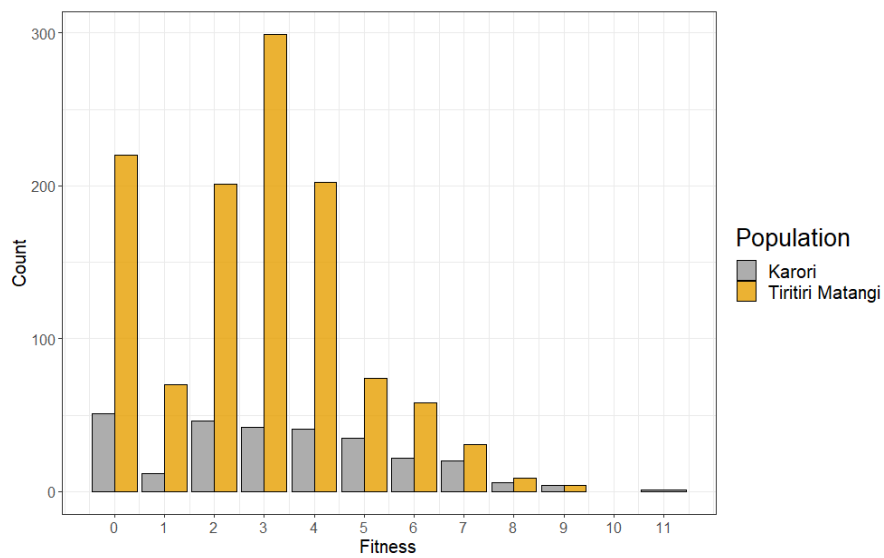


Fig.S.1.b. Fitness (calculated as the number of fledglings produced by each female over one season) in Tiritiri Mātangi and Kārori populations. In both populations, fitness data follow zero-inflated Poisson distributions.

Supplementary Information 2: Power analysis for Kārori

Table S.2: Relative support for models of selection after subsampling the Tiritiri Mātangi dataset. Support is averaged across 10 subsamples of the Tiritiri Mātangi dataset.

Selection model	Relative support (standard error)
ConstOpt	0.193 (0.041)
FluctDir	0.185 (0.051)
FluctCorrDir	0.182 (0.047)
NoSel	0.162 (0.063)
FluctCorrOpt	0.116 (0.024)
FluctOpt	0.109 (0.023)
ConstDir	0.051 (0.012)

With a smaller number of individuals in Kārori (n=168) compared to Tiritiri Mātangi (n=804), models may lack power to distinguish between selective regimes. To test this, we sub-sampled the Tiritiri Mātangi lay date dataset (total number of breeding attempts= 1204) to match the Kārori sample size (total number of breeding attempts = 606), and tested the fit of all models to this dataset.

The support for each model was computed by transforming the LOOIC in model weight in a similar fashion to Akaike weight, i.e.:

$$w_i = \exp(-0.5 * \Delta LOOIC_i) / \sum(\exp(-0.5 * \Delta LOOIC)).$$

Across 10 replicate samples, we found comparable support for all models of directional (42%) or stabilizing selection (42%), the model with no selection receiving the lowest support (16%) (See Table S2). We hypothesise that model fitting is sensitive to the random presence or absence of early reproductions in the dataset, hence smaller sample sizes do not correctly represent the reality of the Tiritiri Mātangi dataset and fail to detect trends observed with the full dataset (See Fig.S2).

In contrast to Kārori (Fig.S1), a close examination of the predicted shape of the models clearly suggests the presence of an optimum (Fig.S2, right panel), and not directional selection (Fig.S1, left panel).

Overall, these analyses suggest that the sample size for Kārori is well-powered to detect directional selection when present.

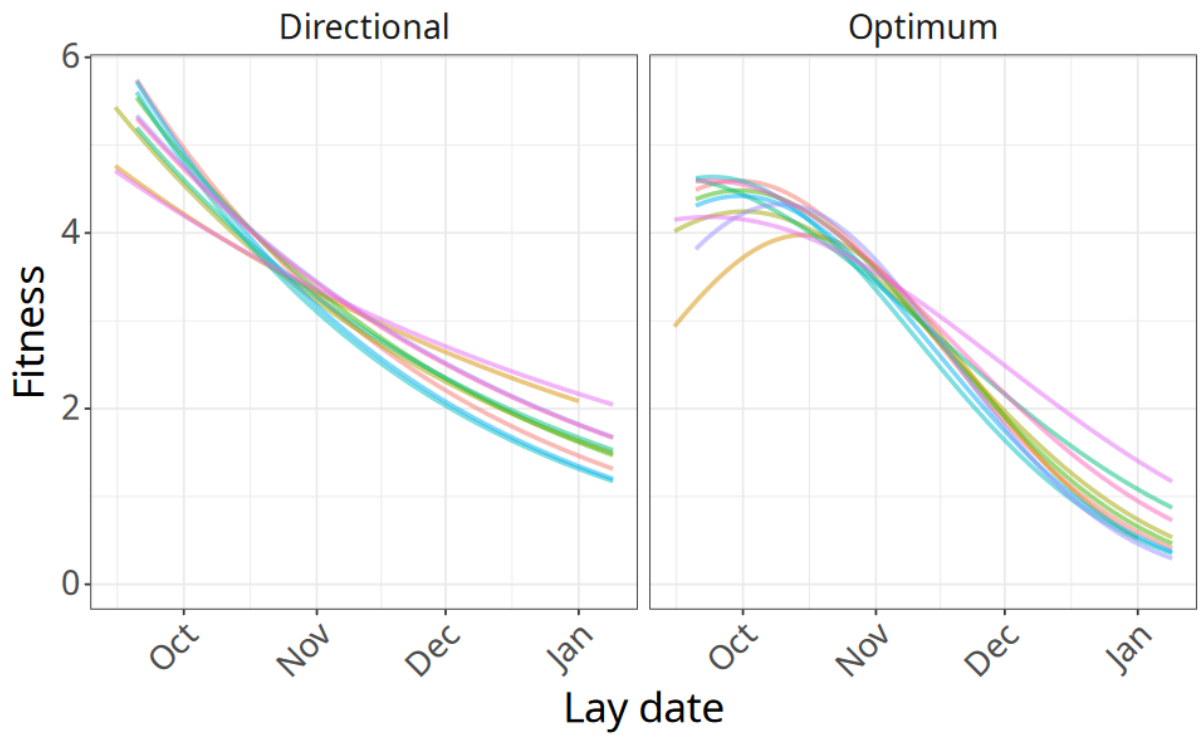


Figure S.2.a: comparison of directional (ConstDir) and optimum (ConstOpt) models in a Tiritiri Mātangi dataset sampled to the same size as Kārori. Each colour represents one of the ten sub-samples.

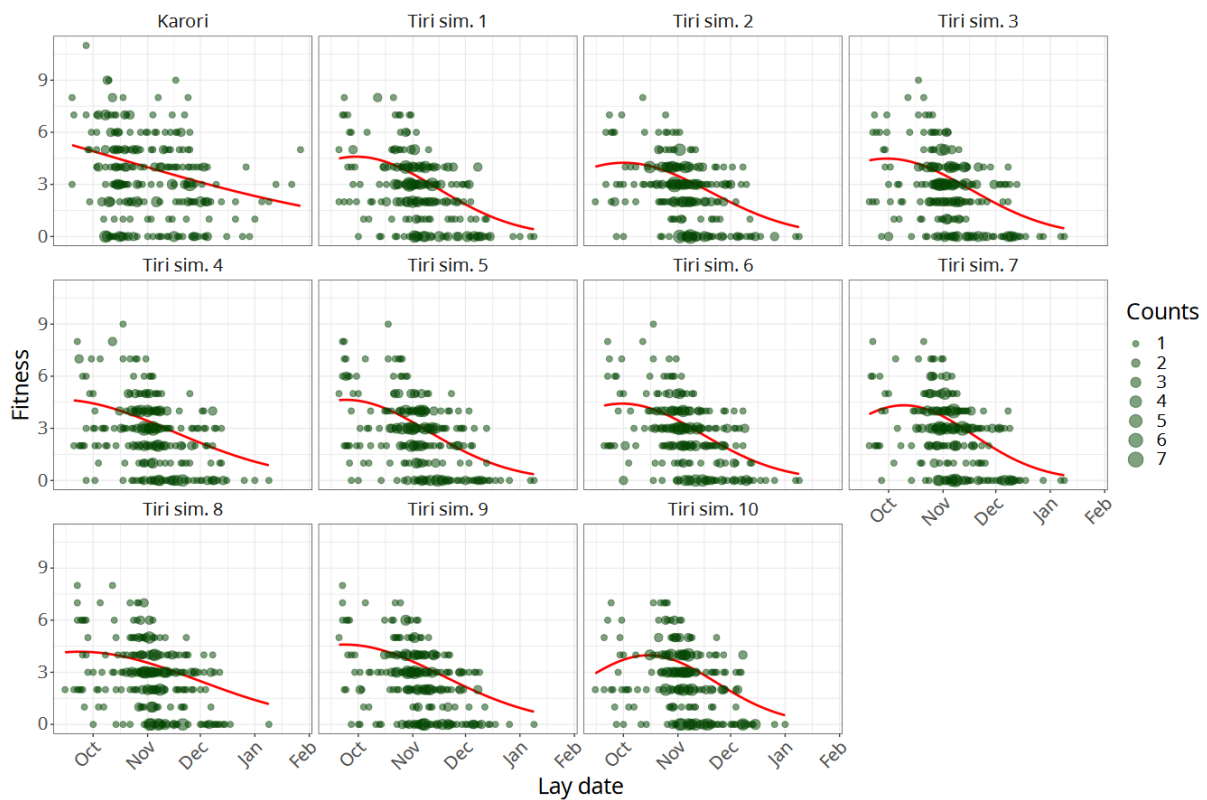


Figure S.2.b – Graphical results of the power analyses. We found support for directional selection in the Kārori population (top left panel) where both the *Dir.* (not represented here) and the *Opt.* models (red curve) are characterized by a linear trend. In contrast, although stabilizing selection was the best supported model in only half of the simulations performed in our power analyses (panels 2 to 11), all the *Opt.* models for sub-sampled Tiritiri Matangi datasets (red curves) display an optimum shape (i.e., a peak). These two findings provide reassurance for the results found for Kārori.

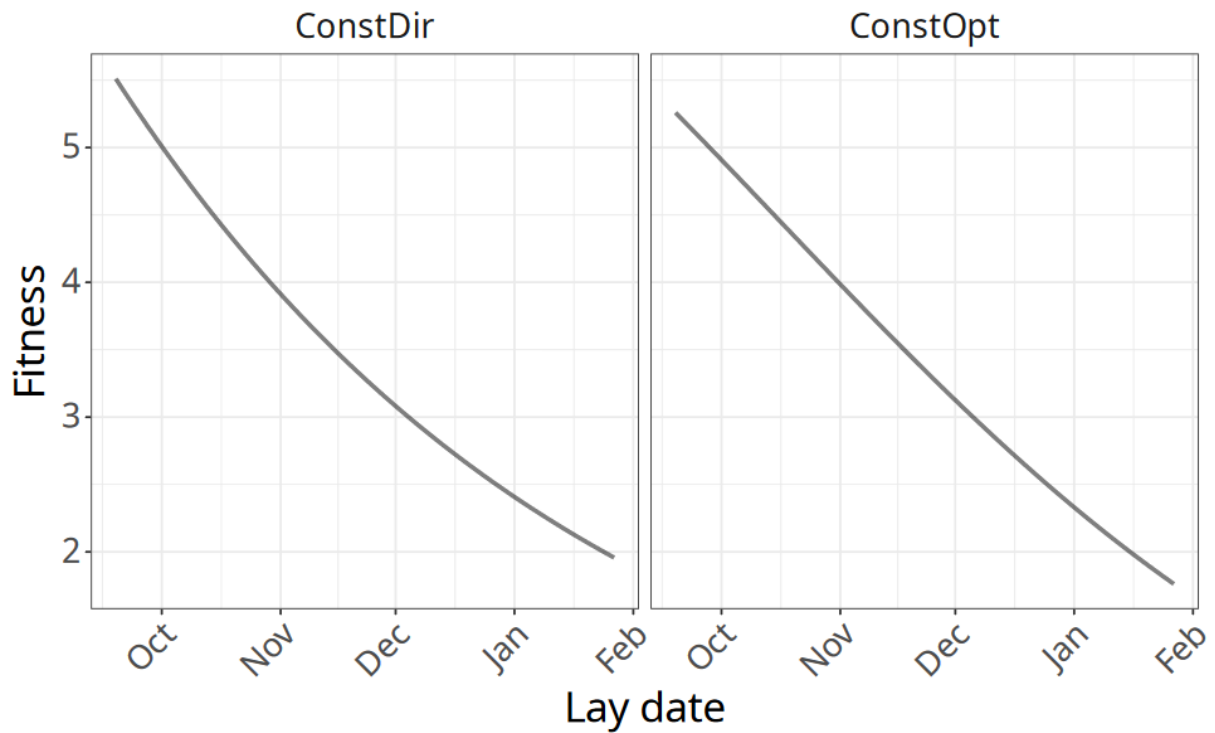


Figure S.2.c: comparison of directional (ConstDir) and optimum (ConstOpt) models in Kārori

In the Kārori population, our results provide mixed support for the shape of the election the shape of selection (stabilizing vs directional; See Table 1). However, a closer comparison of the directional model (ConstDir) and the model with an optimum (ConstOpt) reveals that the inferred shape is also largely directional (no clear optimum is visible), and very similar to the purely directional model, providing support for directional selection.

Supplementary Information 3: Models Estimates

See Tables S3.a-c for Tiritiri Mātangi models and Tables S3.d-f for Kārori.

		Tiritiri Mātangi – No selection					
a.	No Selection	NoSel					
		Parameter	Median	Mode	SE	Low	Up
		Intercept	1.29	1.28	0.0415	1.2	1.36
		St. Dev. Of the intercept	0.143	0.133	0.0374	0.0785	0.223
		Female identity	0.129	0.12	0.0402	0.0347	0.198
		Young	-0.408	-0.397	0.0461	-0.498	-0.315
		Old	-0.489	-0.474	0.125	-0.745	-0.258
		Probability of ZI values (p_{zi})	0.125	0.121	0.0132	0.0999	0.152

		Tiritiri Mātangi – ConstDir					
b.	directional selection	Parameter	Median	Mode	SE	Low	Up
		Intercept	1.17	1.16	0.0366	1.09	1.24
		St. Dev. Of the intercept	0.0979	0.093	0.0341	0.0333	0.169
		Slope (b)	-0.202	-0.2	0.0212	-0.247	-0.163
		Female identity	0.0833	0.0918	0.0414	9.09e-4	0.149
		Young	-0.268	-0.253	0.047	-0.359	-0.175
		Old	-0.363	-0.351	0.119	-0.606	-0.139
		Probability of ZI values (p_{zi})	0.0997	0.098	0.0134	0.0747	0.126
		Tiritiri Mātangi – Fluctdir					
		Parameter	Median	Mode	SE	Low	Up
		Intercept	1.16	1.15	0.0353	1.09	1.23
		St. Dev. Of the intercept	0.0795	0.0823	0.0372	6.4e-4	0.142
		Slope (b)	-0.247	-0.253	0.0388	-0.327	-0.176
		St. Dev. Of the slope (σ_b)	0.133	0.129	0.0353	0.0702	0.208
		Female identity	0.0787	0.061	0.0415	3.18e-5	0.146
		Young	-0.258	-0.262	0.0468	-0.347	-0.165
		Old	-0.364	-0.376	0.118	-0.603	-0.146
		Probability of ZI values (p_{zi})	0.0927	0.0928	0.0132	0.0668	0.118
		Tiritiri Mātangi – Fluctcorrdir					
		Parameter	Median	Mode	SE	Low	Up
		Intercept	1.16	1.15	0.035	1.08	1.22
		St. Dev. Of the intercept	0.0791	0.0698	0.036	0.00425	0.144
		Slope (b)	-0.249	-0.243	0.032	-0.311	-0.184
		St. Dev. Of the slope (σ_b)	0.138	0.126	0.0545	0.06	0.247
Auto-correlation (ϕ)	-0.551	-0.658	0.247	-0.95	-0.0407		
Female identity	0.0776	0.0899	0.0413	3.82e-5	0.145		

Young	-0.256	-0.273	0.0481	-0.354	-0.166
Old	-0.364	-0.331	0.116	-0.599	-0.147
Probability of ZI values (p_{zi})	0.0921	0.0959	0.0132	0.0664	0.118

c.	stabilizing section	Tiritiri Mātangi – ConstOpt					
		Parameter	Median	Mode	SE	Low	Up
		Intercept	1.51	1.51	0.0532	1.41	1.62
		St. Dev. Of the intercept	0.0958	0.0798	0.033	0.0344	0.167
		Omega (ω)	2.83	2.7	0.274	2.39	3.41
		Theta (Θ)	-2.13	-2.02	0.38	-2.93	-1.56
		Female identity	0.0886	0.104	0.0426	5.42e-5	0.154
		Young	-0.268	-0.255	0.0469	-0.36	-0.179
		Old	-0.38	-0.417	0.12	-0.611	-0.142
		Probability of ZI values (p_{zi})	0.0883	0.0862	0.0124	0.0635	0.111
		Tiritiri Mātangi – FluctOpt					
		Parameter	Median	Mode	SE	Low	Up
		Intercept	1.5	1.5	0.0435	1.42	1.59
		St. Dev. Of the intercept	0.0737	0.073	0.0396	2.62e-5	0.143
		Omega (ω)	2.47	2.37	0.249	2.06	2.97
		Theta (Θ)	-1.81	-1.73	0.308	-2.42	-1.26
		St. Dev of theta ($\sigma\Theta$)	0.404	0.376	0.142	0.139	0.708
		Female identity	0.0904	0.0997	0.0425	6.6e-4	0.155
		Young	-0.266	-0.281	0.0471	-0.36	-0.178
		Old	-0.371	-0.355	0.115	-0.599	-0.146
		Probability of ZI values (p_{zi})	0.0828	0.0826	0.013	0.0574	0.109
		Tiritiri Mātangi – FluctCorrOpt					
		Parameter	Median	Mode	SE	Low	Up
		Intercept	1.49	1.5	0.0441	1.41	1.58
		St. Dev. Of the intercept	0.0831	0.0909	0.0405	2.42e-4	0.152
		Omega (ω)	2.4	2.38	0.223	2.01	2.86
		Theta (Θ)	-1.75	-1.7	0.268	-2.28	-1.28
		St. Dev of theta ($\sigma\Theta$)	0.445	0.452	0.221	0.0889	0.879
		Auto-correlation (ϕ)	-0.564	-0.583	0.324	-0.985	0.126
		Female identity	0.0911	0.088	0.0419	0.00157	0.156
Young	-0.266	-0.259	0.0465	-0.351	-0.173		
Old	-0.37	-0.358	0.116	-0.609	-0.163		
Probability of ZI values (p_{zi})	0.0822	0.084	0.0126	0.0599	0.109		

d.	Kārori - NoSel						
	No Selection	NoSel					
		Parameter	Median	Mode	SE	Low	Up
		Intercept	1.39	1.41	0.076	1.24	1.54
		St. Dev. Of the intercept	0.167	0.167	0.0755	0.00605	0.304
		Female identity	0.189	0.196	0.0637	0.0531	0.309
		Young	-0.0734	-0.0764	0.0818	-0.228	0.0873
		Old	-0.432	-0.463	0.488	-1.41	0.453
Probability of ZI values (p_{zi})		0.157	0.154	0.0245	0.114	0.21	

e.	Kārori – ConstDir						
	Parameter	Median	Mode	SE	Low	Up	
	Intercept	1.36	1.35	0.0604	1.25	1.48	
	St. Dev. of the intercept	0.0685	0.0233	0.0535	6.20E-06	0.174	
	Slope (b)	-0.151	-0.15	0.0343	-0.22	-0.0852	
	Female identity	0.168	0.178	0.0625	0.031	0.281	
	Young	-0.039	-0.023	0.0759	-0.187	0.11	
	Old	-0.501	-0.51	0.495	-1.52	0.403	
	Probability of ZI values (p_{zi})	0.157	0.155	0.0246	0.109	0.204	
	directional selection	Kārori – Fluctdir					
		Parameter	Median	Mode	SE	Low	Up
		Intercept	1.37	1.37	0.0604	1.24	1.48
		St. Dev. Of the intercept	0.0618	0.00747	0.0508	2.49E-04	0.166
		Slope (b)	-0.15	-0.144	0.0376	-0.223	-0.0745
		St. Dev. Of the slope (σ_b)	0.0449	0.00683	0.0394	8.58E-05	0.125
		Female identity	0.168	0.189	0.0613	0.0326	0.275
		Young	-0.0528	-0.0365	0.0769	-0.204	0.0941
		Old	-0.53	-0.328	0.494	-1.51	0.374
		Probability of ZI values (p_{zi})	0.157	0.161	0.0243	0.109	0.205
		Kārori – Fluctcorrdir					
		Parameter	Median	Mode	SE	Low	Up
		Intercept	1.37	1.37	0.0597	1.25	1.48
		St. Dev. Of the intercept	0.0607	0.0428	0.052	2.95E-05	0.167
		Slope (b)	-0.151	-0.161	0.0411	-0.223	-0.0677
	St. Dev. Of the slope (σ_b)	0.0448	0.00208	0.0467	5.98E-05	0.14	
	Auto-correlation (ϕ)	-0.224	-0.541	0.479	-0.967	0.672	
	Female identity	0.169	0.19	0.0618	0.0281	0.274	
Young	-0.053	-0.0298	0.0771	-0.203	0.0957		
Old	-0.515	-0.399	0.485	-1.48	0.371		
Probability of ZI values (p_{zi})	0.157	0.158	0.0237	0.112	0.203		

f.

stabilizing selection	Kārori – ConstOpt					
	Parameter	Median	Mode	SE	Low	Up
	Intercept	2.04	1.75	0.795	1.35	3.85
	St. Dev. Of the intercept	0.0694	0.0425	0.0563	3.21E-05	0.182
	Omega (ω)	7.98	7.54	2.7	4	13.8
	Theta (Θ)	-9.08	-5.53	8.71	-28.8	-1.09
	Female identity	0.167	0.189	0.063	0.0221	0.276
	Young	-0.0384	-0.0133	0.0758	-0.197	0.0993
	Old	-0.518	-0.471	0.482	-1.54	0.328
	Probability of ZI values (p_{zi})	0.158	0.166	0.0242	0.114	0.207
	Kārori – FluctOpt					
	Parameter	Median	Mode	SE	Low	Up
	Intercept	1.87	1.67	0.599	1.38	3.16
	St. Dev. Of the intercept	0.0676	0.0266	0.058	9.86E-06	0.185
	Omega (ω)	7.35	6.99	2.46	3.61	12.7
	Theta (Θ)	-7.14	-5.37	6.83	-22.4	-0.889
	St. Dev of theta ($\sigma\Theta$)	0.412	0.0795	0.476	4.26E-05	1.44
	Female identity	0.165	0.169	0.0638	0.018	0.271
	Young	-0.0461	-0.0529	0.0764	-0.189	0.104
	Old	-0.489	-0.282	0.487	-1.54	0.365
	Probability of ZI values (p_{zi})	0.156	0.156	0.0238	0.111	0.205
	Kārori – FluctCorrOpt					
	Parameter	Median	Mode	SE	Low	Up
	Intercept	1.88	1.64	0.589	1.4	3.3
	St. Dev. Of the intercept	0.0723	0.00236	0.0586	7.40E-05	0.19
	Omega (ω)	7.46	6.78	2.47	3.97	12.9
	Theta (Θ)	-7.32	-4.61	6.85	-23.4	-0.962
St. Dev of theta ($\sigma\Theta$)	0.427	0.0373	0.56	3.25E-04	1.62	
Auto-correlation (ϕ)	-0.198	-0.584	0.465	-0.968	0.67	
Female identity	0.164	0.153	0.0622	0.0306	0.279	
Young	-0.0491	-0.0272	0.0776	-0.196	0.105	
Old	-0.521	-0.365	0.489	-1.55	0.358	
Probability of ZI values (p_{zi})	0.158	0.16	0.0243	0.109	0.206	

Supplementary Information 4: Comparison of Tiritiri Mātangi and Kārori's environments.

Tiritiri Mātangi sanctuary is located on an offshore island in Tikapa Moana / Hauraki Gulf (36°36'8"S, 174°53'13"E), a sub-tropical climatic zone. The Kārori population is located in Zealandia urban eco-sanctuary, within Wellington city (41°17'26"S, 174°45'10"E). This region is exposed to Cook Strait meteorological conditions and, compared to Tiritiri Mātangi is situated within an oceanic climatic zone. To describe the average environmental conditions prior to breeding, we first calculated the grand mean of the start of the breeding season across years in each population. We then compared the average ambient temperature and amount of precipitation recorded over the 35 days prior to this date (See Supplementary Information 5 for a justification of this timing). Data were downloaded from the New Zealand National Climate Database (<https://cliflo.niwa.co.nz>; "Tiritiri Mātangi Lighthouse" and "Wellington, Kelburn Aws" stations for Tiritiri Mātangi and Kārori, respectively).

Student tests revealed a significant difference between the average temperature recorded over the 30 days before the grand mean start of the breeding season, Tiritiri Mātangi habitat being approximately 20% warmer than Kārori (Tiritiri Mātangi: $17.21 \pm 0.46^\circ\text{C}$ Kārori: $14.49 \pm 0.71^\circ\text{C}$; $t_{24,31} = -12.3$; $p\text{-value} < 0.001$; Fig.S.6). Similarly, we found a significant difference in the amount of precipitation, Tiritiri Mātangi being almost 70% drier than Kārori (Tiritiri Mātangi: $78.37 \pm 25.06\text{ mm}$; Kārori: $131.73 \pm 61.25\text{ mm}$; $t_{24,36} = -12.3$; $t_{18,21} = 3.11$; $p\text{-value} = 0.006$; Fig.S3.c).

Interestingly, the minimum temperatures recorded in Tiritiri seems to be always warmer than the warmest temperatures recorded in Kārori. This difference could be explained by the latitude difference between both populations (more than 500km separates them, See Fig.1 of the main manuscript). Also note that Tiritiri Mātangi Island is located in Hauraki Gulf, while Zealandia Sanctuary (hosting the Kārori population) is located in a valley within Wellington and exposed to the Cook Strait climatic conditions.

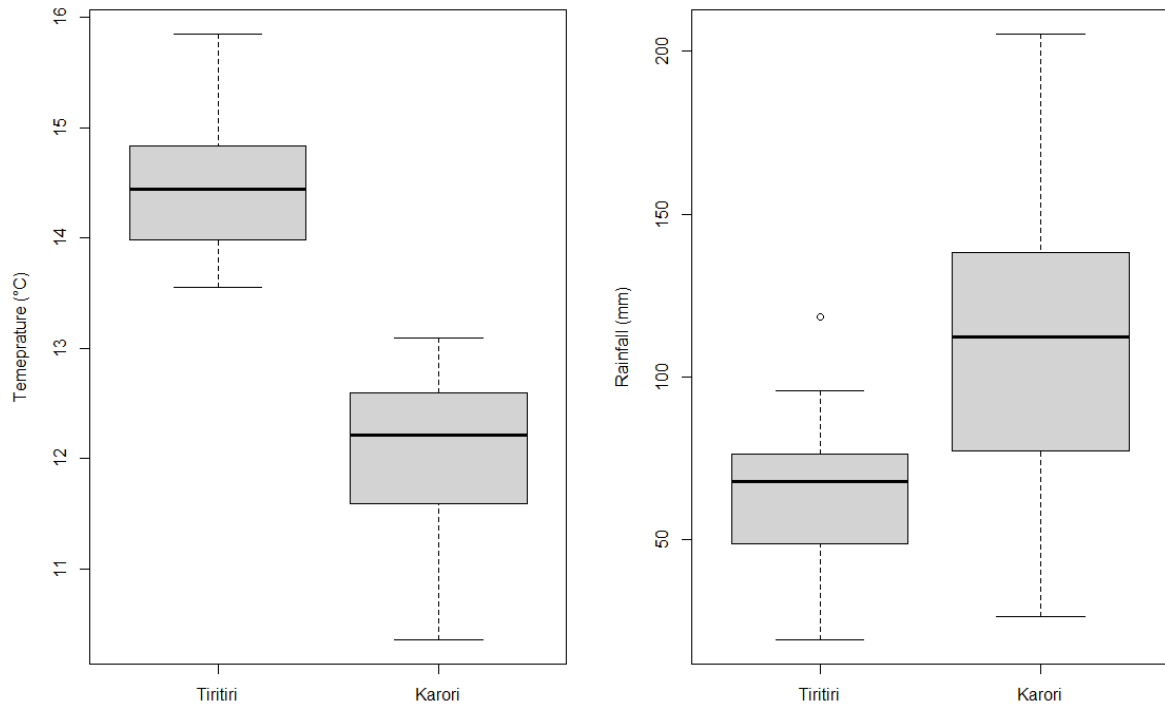


Fig.S.4 Comparison of average temperature and rainfall amount between Tiritiri Mātangi and Kārori. Both temperatures (left panel) and rainfall amounts (right panel) are recorded during a 30 days' time-window preceding the average start of the breeding season.

Supplementary Information 5: Relationship between environmental conditions and laying date in the hihi

To check the existence of phenotypic plasticity in laying date in response to environmental cues, we explored the relationship between different parameters of environmental conditions and the start of the breeding season. More specifically, we used a sliding-window method to test temperature and precipitation as potential cues for the start of breeding season (Brommer, Rattiste, & Wilson, 2008). For each site, the grand mean of the start of the breeding season across years was correlated to the average ambient temperature and amount of precipitation recorded over twelve temporal windows preceding the start of the breeding season (ranging from 5 to 60 days, with an increment of five days). Data were downloaded from the New Zealand National Climate Database (<https://cliflo.niwa.co.nz>).

1. Tiritiri Mātangi

Unfortunately, the weather forecast was only recorded on the island until 2010 and after 2015 (Tiritiri Mātangi Lighthouse Station), as the station was closed for several years. As a consequence, we could only use the data for 18 seasons (from 1997 to 2010 and 2016 to 2020), the next closest station (Whangaparaoa Aws) being situating on the mainland, 5.8 km away.

First, for each time window, we performed a linear regression between the environmental cue (Temperature (T) and Rainfall (RF)) recorded over the specific time window and the annual average date of breeding season. Second, in an attempt to better understand the relationship between temperature and rainfall, we also performed a linear regression between the two parameters. Because we performed multiple tests, we used a Bonferroni correction to take into account the probability to reject the null hypothesis by chance. Specifically, as we used twelve time-windows (and therefore performed twelve tests on each data sets), we chose a significance cut-off for the p-value at 0.004 (0.05/12). Model coefficients and p-values are reported in Table S5.a.

Our results suggest a clear association between temperature and the start of the breeding season (see Figure S5.a), the warmer the period (and the longer the warm period) before the grand mean of the start of the breeding season across years, the earlier the start of the season. This result is not surprising and was already found by de Villemereuil et al. (2019). We found no support for a relationship between the start of the breeding season and the amount of precipitation, and temperature and precipitations seem uncorrelated in this population.

Table S5.a Relationship between start of the breeding season and Temperature or Rainfall in Tiritiri Mātangi. Provided are the coefficients and p-value of linear regressions between the start of the breeding season and Temperature (T) or rainfall (RF) recorded over twelve temporal windows. After Bonferroni correction, significant p-values are provided in blue.

Temporal window	Temperature		Rainfall		T-RF	
	Coefficient	p-value	Coefficient	p-value	Coefficient	p-value
5 days	-5.2124	0.0046	-0.4786	0.0969	0.0317	0.3825
10 days	-6.9765	0.0014	-0.1122	0.5689	-0.0087	0.6581
15 days	-9.5142	0.0000	-0.1421	0.1624	0.0104	0.2396
20 days	-10.8325	0.0003	0.0075	0.9424	0.0047	0.5149
25 days	-9.4125	0.0012	-0.0903	0.3471	0.0092	0.1935
30 days	-8.6527	0.0013	-0.0440	0.6087	0.0073	0.2856
35 days	-8.8344	0.0021	-0.0004	0.9956	0.0028	0.6395
40 days	-8.6655	0.0057	0.0463	0.4214	-0.0004	0.9265
45 days	-9.2024	0.0045	0.0288	0.5740	-0.0010	0.7717
50 days	-9.5078	0.0033	0.0053	0.8982	0.0001	0.9643
55 days	-10.3620	0.0046	0.0145	0.7340	-0.0012	0.6405
60 days	-10.5982	0.0048	0.0266	0.5244	-0.0015	0.5525

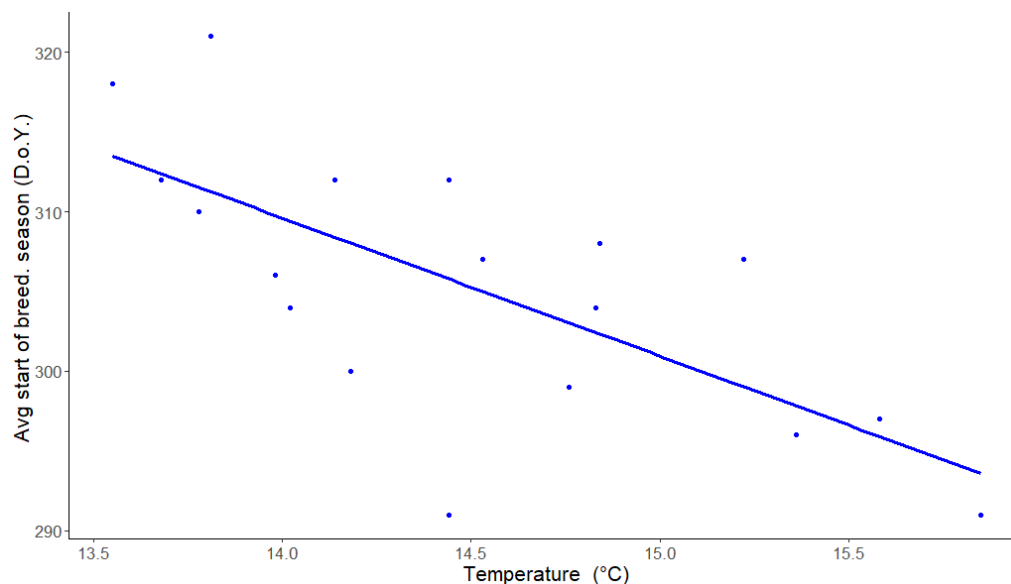


Figure S5.a Relationship between temperature and average start of the breeding season in Tiritiri Mātangi, for a time-window of 30 days. The significant relationship suggests a plastic response of laying date to temperature, the warmer the environment, the earlier the breeding.

2. Kārori

We used a similar approach in Kārori, using the “Wellington, Kelburn Aws” weather forecast station located ~2 km away from the sanctuary. Again, we tested the relationship between temperature (T) and amount of rainfall (RF) and the start of the breeding session. We also tested the relationship between T and RF. Again, we applied a Bonferroni correction to the p-value cut-off threshold. Results are summarized in Table S5.b.

In contrast to Tiritiri Mātangi, we found no association between environmental parameters and the start of the breeding season across years, suggesting a lack of climatic-based plastic response (See Figure S5.b). Yet, we found significant and negative correlations between temperature and rainfall for three temporal windows tested, suggesting that the most humid years are also the coldest.

Table S5.b Relationship between start of the breeding season and Temperature or Rainfall in Kārori. Provided are the coefficients and p-value of linear regressions between the start of the breeding season and Temperature (T) or rainfall (RF) recorded over twelve temporal windows. After Bonferroni correction, significant p-values are provided in blue.

Temporal window	Temperature		Rainfall		T-RF	
	Coefficient	p-value	Coefficient	p-value	Coefficient	p-value
5 days	0.2462	0.9148	0.0829	0.6988	-0.0265	0.3054
10 days	0.2462	0.8406	-0.0067	0.9482	-0.0136	0.1107
15 days	0.2462	0.9488	0.0083	0.9320	-0.0148	0.0458
20 days	0.2462	0.8969	-0.0108	0.9113	-0.0099	0.0875
25 days	0.2462	0.6277	-0.0335	0.6329	-0.0133	0.0002
30 days	0.2462	0.5448	-0.0600	0.3651	-0.0131	0.0005
35 days	0.2462	0.3967	-0.0386	0.5062	-0.0100	0.0007
40 days	0.2462	0.4065	-0.0472	0.3973	-0.0077	0.0051
45 days	0.2462	0.4199	-0.0304	0.6160	-0.0054	0.0612
50 days	0.2462	0.4137	-0.0213	0.7138	-0.0046	0.0756
55 days	0.2462	0.4136	-0.0134	0.8112	-0.0032	0.1823
60 days	0.2462	0.4207	-0.0258	0.6384	-0.0028	0.2120

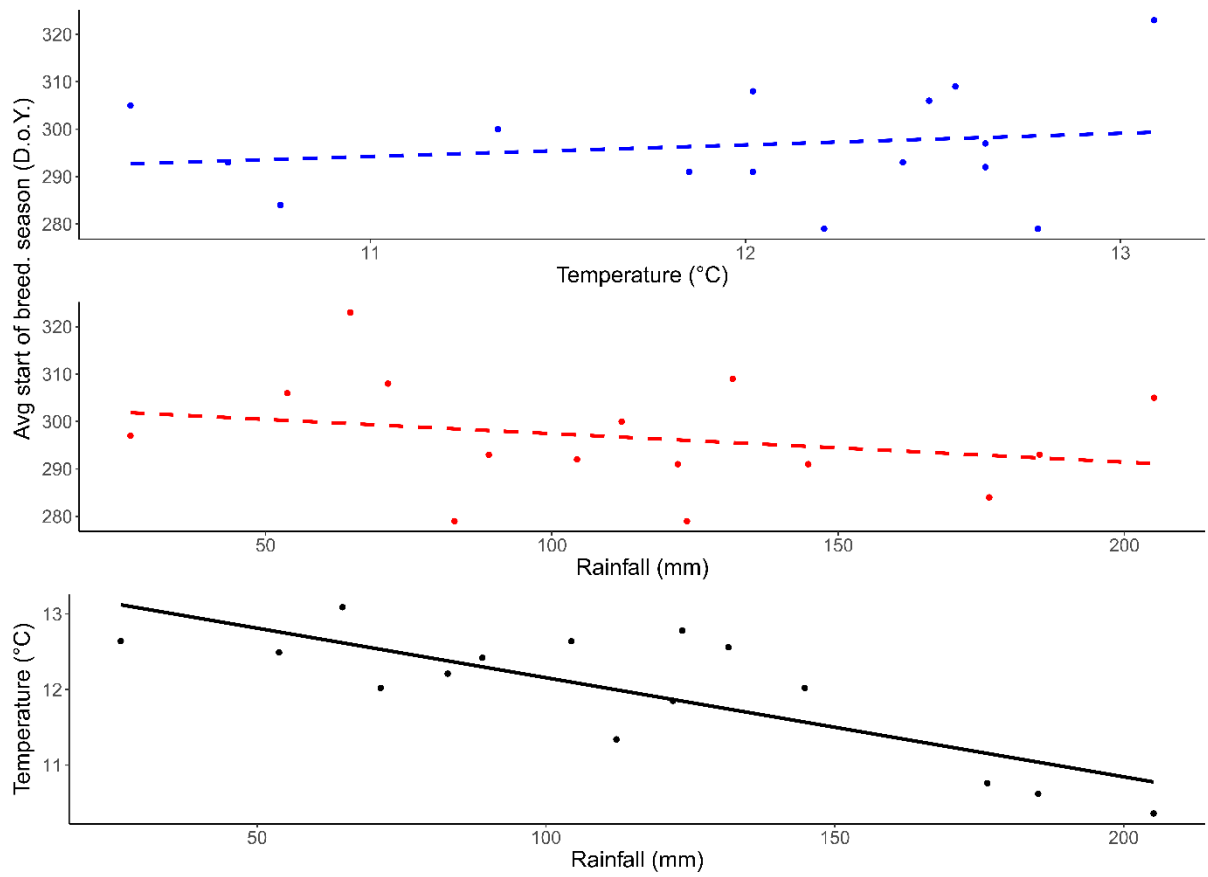


Figure S5.b Relationship between environmental parameters and the average start of the breeding season in Kārori, for a time-window of 30 days. Top panel represents the relationship between temperatures and the **average start of the breeding** season. Middle panel represents the relationship between the total amount of rainfall and the **average start of the breeding** season. The bottom panel represents the relationship between temperature and total rainfall. Significant relationships are represented with solid lines.